

SUPPLEMENTARY INFORMATION FOR “Pulsed glucocorticoid administration enhances dystrophic muscle performance through epigenetic and metabolic reprogramming by Quattrocchi et al.

Supplemental Table 1. Biomarkers of obesity and metabolic syndrome in DMD patients receiving daily compared to weekend glucocorticoids (CG).

	daily GC regimen	weekend GC regimen	
<i>MEASUREMENTS</i>	<i>mean ± s.e.m</i>	<i>mean ± s.e.m</i>	<i>P value</i>
age (years)	10.92 ± 0.92	9.59 ± 0.82	0.199
treatment duration (months)	54.92 ± 6.94	47.17 ± 7.74	0.417
height (cm)	129.07 ± 4.33	137.09 ± 6.6	0.217
weight (kg)	36.6 ± 3.65	43.46 ± 8.63	0.377
BMI (kg/m ²)	21.89 ± 1.72	21.77 ± 2.59	0.963
fat mass TBLH (%)	50.36 ± 3.07	36.28 ± 3.61	0.002
lean mass TBLH (%)	48.19 ± 3.94	64.93 ± 4.19	0.002
BMD TBLH (Z-score)	-2.92 ± 0.22	-1.2 ± 0.26	<0.001
BMD L1-L4 (Z-score)	-2.13 ± 0.28	-0.34 ± 0.25	<0.001
<i>SERUM</i>			
cortisol (ng/ml)	2.76 ± 0.54	15.4 ± 3.65	0.001
glucose (mg/dl)	126.67 ± 7.25	105.25 ± 3.69	0.005
insulin (ng/ml)	3.1 ± 0.79	0.64 ± 0.16	0.003
BCAA (μM)	633 ± 31.8	492 ± 31.3	0.005
free fatty acids (μM)	402.62 ± 9.03	361.86 ± 8.87	0.004
<i>MOBILITY and MUSCLE DAMAGE</i>			
Brooke's score (AU)	6.00 ± 1.10	5.25 ± 1.14	0.571
10m run test (sec)	(n=5) 7.5 ± 0.57	(n=7) 6.7 ± 1.07	0.785
creatine kinase (U/L)	12626 ± 3448	17770 ± 4850	0.312
<i>HEART FUNCTION</i>			
PR interval (msec)	113.45 ± 2.87	118.55 ± 5.32	0.339
QRS interval (msec)	83.09 ± 3.11	77.64 ± 3.01	0.202
QT interval (msec)	336.36 ± 9.20	337.09 ± 10.09	0.951
LV septum thickness (cm)	0.70 ± 0.04	0.69 ± 0.06	0.917
LV PW thickness (cm)	0.73 ± 0.04	0.70 ± 0.05	0.592
fractional shortening (%)	31.49 ± 1.35	32.05 ± 0.90	0.786

Supplemental Table 2. List of regulatory regions identified through H3K27ac ChIP-seq analysis, and targeted for ChIP-qPCR assays.

Gene	Regulatory region	H3K27ac peak region (mm10)	target element sequence
<i>Klf15</i>	<i>GRE</i>	chr6:90462191-90464692	TGGGACACCATGTTC
<i>Klf15</i>	<i>KRE</i>	chr6:90470011-90472892	TGGGGGGTGGGGTGC
<i>Klf15</i>	<i>MEF2</i>	chr6:90461636-90478713	ACTAAAAATAGC
<i>Mef2c</i>	<i>GRE</i>	chr13:83522844-83528432	TCACAGACTGTTCTG
<i>Mef2c</i>	<i>KRE</i>	chr13:83517868-83518938	AGACCCCGCCCTCC
<i>Mef2c</i>	<i>MEF2</i>	chr13:83570825-83576273	GTTATTTTTACT
<i>Bcat1</i>	<i>GRE</i>	chr6:144909891-144910938	AAAAACAAATGTTC
<i>Bcat1</i>	<i>KRE</i>	chr6:144909891-144910938	CAGTCCACCCCTAA
<i>Bcat1</i>	<i>MEF2</i>	chr6:144909891-144910938	ACCAAAAAATAGG
<i>Bckdha</i>	<i>GRE</i>	chr7:25651075-25652652	GAACAGACAGTGCTC
<i>Bckdha</i>	<i>KRE</i>	chr7:25655965-25660179	CTGGGGGTGGGGTGG
<i>Bckdha</i>	<i>MEF2</i>	chr7:25649671-25650527	TTTATTTTTATT
<i>Glud1</i>	<i>GRE</i>	chr14:34313334-34314182	CAACAGATTGTTCTG
<i>Glud1</i>	<i>KRE</i>	chr14:34309498-34312292	TAGCCCCGCCCCCGC
<i>Glud1</i>	<i>MEF2</i>	chr14:34309044-34319109	TCCTAAAAATAAA
<i>Got1</i>	<i>GRE</i>	chr19:43521165-43529588	TTGGACACACTGTAC
<i>Got1</i>	<i>KRE</i>	chr19:43510300-43513519	TAGCCCCGCCCTCCC
<i>Got1</i>	<i>MEF2</i>	chr19:43521165-43529588	AACAGAAATAGC
<i>Gpt2</i>	<i>GRE</i>	chr8:85492357-85493740	GCAGTGCCTGTCCC
<i>Gpt2</i>	<i>KRE</i>	chr8:85519705-85525024	GTGCCCCACCCCCCT
<i>Gpt2</i>	<i>MEF2</i>	chr8:85511283-85517802	AATAAAAAAATAC
<i>Deptor</i>	<i>GRE</i>	chr15:55134099-55135703	AAGAACGATGTGTTC
<i>Deptor</i>	<i>KRE</i>	chr15:55131703-55133628	AGCAGGGTGGGGTGT
<i>Deptor</i>	<i>MEF2</i>	chr15:55131703-55133628	TTTATTTTTGAT
<i>Ldha</i>	<i>GRE</i>	chr7:46825852-46834466	GAGTACATAATGCTC
<i>Ldha</i>	<i>KRE</i>	chr7:46837370-46840203	CTACCCACCCCCGC
<i>Ldha</i>	<i>MEF2</i>	chr7:46844401-46847654	TTCAAAAAATAGA
<i>Pck1</i>	<i>GRE</i>	chr2:173157052-173157552	CAGGACGGTGAGTCC
<i>Pck1</i>	<i>KRE</i>	chr2:173157052-173157552	CCTGGGGTGTGGCGA
<i>Pcx</i>	<i>KRE</i>	chr19:4509355-4511511	CGAGGGCGGAGTCG
<i>Pcx</i>	<i>MEF2</i>	chr19:4535136-4535636	ACCATATATAGC
<i>Pfkm</i>	<i>GRE</i>	chr15:98111107-98117349	GAACACAGCGTCCCC
<i>Pfkm</i>	<i>KRE</i>	chr15:98108180-98110085	GAGCTACACCCAACC
<i>Pfkm</i>	<i>MEF2</i>	chr15:98108395-98110085	TTTATATTTAGC
<i>Smarcd3</i>	<i>GRE</i>	chr5:24600248-24605130	GGAACAGACAGTTC
<i>Smarcd3</i>	<i>KRE</i>	chr5:24598194-24599265	GGGGGGGCGGAGTTT
<i>Smarcd3</i>	<i>MEF2</i>	chr5:24600248-24605130	TCTATTTCTGGG
<i>Adipoq</i>	<i>GRE</i>	chr16:23163366-23168343	GGGCACAGGTTGTTC
<i>Adipoq</i>	<i>KRE</i>	chr16:23180995-23183171	GGGAGGGTGGGGTGG
<i>Adipoq</i>	<i>MEF2</i>	chr16:23176392-23177054	TTTATTTTAAAC
<i>Adipor2</i>	<i>GRE</i>	chr6:119376615-119378483	TCACATAATGTACTG
<i>Adipor2</i>	<i>KRE</i>	chr6:119416203-119420293	CAGTGGGCGTGGCCT
<i>Adipor2</i>	<i>MEF2</i>	chr6:119416203-119420293	AATAAAAAATAAA
<i>Cd36</i>	<i>GRE</i>	chr5:17890487-17895634	AAGAACAGTCAGTGC
<i>Cd36</i>	<i>KRE</i>	chr5:17884000-17889533	CAACTCCGCCCATATA
<i>Cd36</i>	<i>MEF2</i>	chr5:17827696-17838060	ATCCAAAAATAGA
<i>Dgat2</i>	<i>GRE</i>	chr7:99199241-99199968	GAACAGGGTGACCTT
<i>Dgat2</i>	<i>KRE</i>	chr7:99182170-99183833	TATAGGGCGGGGCAA
<i>Dgat2</i>	<i>MEF2</i>	chr7:99201746-99203086	GTTATAAATAAC
<i>Ech1</i>	<i>GRE</i>	chr7:28819366-28821894	GAACAATCGGTTCTC
<i>Ech1</i>	<i>KRE</i>	chr7:28823813-28827057	GTGTGGGTGGGGTGG
<i>Ech1</i>	<i>MEF2</i>	chr7:28823813-28827057	TTTATTTTTATT
<i>Gpd1</i>	<i>GRE</i>	chr15:99717644-99718707	CAGGACAGTCTGTGC
<i>Gpd1</i>	<i>KRE</i>	chr15:99717486-99720976	AGGGGGGCGGAGTGA
<i>Gpd2</i>	<i>GRE</i>	chr2:57236646-57239830	AGAAACACACTGTTC
<i>Gpd2</i>	<i>KRE</i>	chr2:57236646-57239830	TCATGGGTGGAGTAC
<i>Gpd2</i>	<i>MEF2</i>	chr2:57319557-57320057	GTTATTTATATA
<i>Pnpla2</i>	<i>GRE</i>	chr7:141454860-141457616	CAGCACACAAAGTTC
<i>Pnpla2</i>	<i>KRE</i>	chr7:141454860-141457616	GAAGGGGCGGGGCCT
<i>Pnpla2</i>	<i>MEF2</i>	chr7:141452037-141452537	AACAAAAATAGA
<i>Tpi1</i>	<i>KRE</i>	chr6:124812191-124814237	GCTAGGGCGTGGCTC
<i>Tpi1</i>	<i>MEF2</i>	chr6:124812191-124814237	TTCTAAAAATAGC

Supplemental Table 3. Regulatory sequences and transcription factor binding sites for luciferase assays in electroporated myofibers.

transcription factor binding site (position from TSS)	sequence (GRE sites in red; KRE sites in grey; MEF2 sites in blue)
Mef2C GRE-KRE (I intron; +1173bp)	AACTGTGCTTCACAGCATTTCT CTACACATTGTTG TATTATAGCAAATTGAAAACATTTATTTAA GCAAGGAAGCAGCTCAAAGCTAGGGACTATACATAGCAAACATATGAAACCATTTTAATAAGT AAATTCCATATTCACAAGCAACATGGGCTAATGAATGTAAGACACAACGGCATACTTGGT CAAGAATGCTATAAATTATTATGCATTAATAATCAATTTCTGGGCT GTGGGGGTAGG ATTGG TACTTAAGAAGAGAAAAGCTTC
Bckdha GRE-KRE (I intron; +12354bp)	TGAGCTATGGTGTCCAAGCAG GGACACACTGTC AGGGGACCTGATGCAACCATTTCAGATACCC AGGTGGACTTCACATACTGGAGCAGGCACAGACCATGTTCTCCAGTCCCCTCTTTCCAAAGG GCTGCCCTTACCCCCATGAAGTCACTGTGCTAATTCAGTGAGTTCCAAAACCTGGTCAATAATG ACACTGGATGCTGGATTATAGAATGGGCAATAAAATACCTACAGAGGCTGGGCAGTGGTAGT GTACAACCTTTAATCCAGCGCTTGGGAGGCAGAGGCAGGCGGATCTCTGTGGGTTTGAGGC CAGCCTGGTATGCAAAGTGAGTTCCAGGTCAGCCAGGGTGACAGAGAAAC CTCCCCACC CAATCCTACATGTGGTCATATACCTTCTCTGTAGGA
Pfkm GRE-KRE (I intron; +26920bp)	TCGTTTTAGTAGACCCCTCCTTTTCTCTC ACTCCCCACC ACCCCGTGACCCCTGACTTTGC TGTGCACCCCTCTGTTCTCTTCTCCTTTTCATGCCCCCTCCCCATCCTTCATCACCTATTCTCA TCTCTCTTGGTCTCGTCTCTAATTTTAAAGGGTTTACCCACACTTACTCCCGTTCATGCGTATA CAGGTCTACTTTACAGGGTAGGAGCTTCATATGAGAGACAGAGGAAATGTAGTTTTTGTCTTT CTGAGTTTGGGTCACTTAATA CTACACTTTGTAG ATCCATCCATTTTCTAAAAAAAAAAAAA AAGCAATAATTTAGGCTTTTTCTTTATAGCTGAGTAAATCCATTCCATACATGTACCACATT TCCATTACCCA
Ech1 GRE-KRE (promoter; -8017bp)	GAGGTGACCTGGAGTGAGGGCGGTGCTT GGCCACCCCCCTCCG GAACCACACTTCAGCGGCT CTGCCTCTGCACATTGCGCACCAACACACAGGGCACAAAACCACTAGTCTTCCCTGGAGAAC AACATGCAGCCTCCACCACGCTCCCAGAGACAGCCGCAGATTGAGCTCACTACATCAAGAAC ACCACACCGCGCTCCAAGGAACAGCTACAAGCACAGAGACAGAGGCAGACAGAGACAAAGA AAGAGACGCAACATGGCAGCAGACACTGCTTTTTTACTAAACATAAAAAAAGTCAAAAAATCCA AGCAAACCTGAACCCAAGAATGTACACAGAAGTAGGAAACACAGCCCAAGTGCGCCAGCCA GCCAGCGGTGCTCTTTTCGGAGAACGATTGATTGATGAGTGAAGTAGATTCCATGAGCCT CCAAGACAATAGGATCCTCCATTCCTCGCCATGCAGGTTTTGTTTTTTAAGTCCTTTGGTTTG GGGAGGGCCTTCTTTTTTTTCTTTTGATTTTTTGATTTTTTTTTTCTGAGTCATCGGCTGCCA ACACAGTCTGCACCAACTGGAGATCAGAAATAAAAAATTAACCACAACAACAAAAATCAGA AAACAGACCTAAAATCAAACAGCTCAGAGGCACACAGTTACCTGCTGGTGGGTAAACGGGC ACGCAACCAAGGCCACAGCGGAGCATAGTGGGGCCACTGGCACACTTCATACCAGGAGAC ACGCACATGGAGCGCTACACAGCCAGAAGCACCGCACTGC AGCACACAGTGTG AGGAGCTG ACCACACGGAGGGACACTACCCACCTCATAACCTTTATTT
Bckdha MEF2 (promoter; -92bp)	CTTGCGACAAAGACGCATAAATGAGTAAGGT GGCAATTTTTAGT CTCTAAATTGCTCCGGTC GTCTGCTTCTAGTTGCTCCTAATTCAGGCAACTAAAGGACAACCTTAACCTGAACCTTCAGGG TTCAGGACCCGGAGCCCTGAGCAAAATGGGCCCTCTCCAAGTCCCTCCCCCTGTTCCCTGTT GTCCAATGGCTATGCCAGAATTGG
Pfkm MEF2 (promoter; -736bp)	TGGACTCTCTCCCCAGTTAAATAGTACCTTAAGCACCTTACTATTCTAACCTTTAAATAGTA CTTAACCTCTTACACACATACACTAAGTGTGGGGTTCTGGGATATAAACACAAGAAAGCTCTG GCCTTTGCCCTTTAGTAGTTTTTCAAGCCAGGCGAGGAAGCCAGATCCAGTCA
Ech1 MEF2 (promoter; -2200bp)	GGACCTGCTGAGTGTTGTGTGTGTGTGTGTGTGTGTGTGTATGTATGTGTATGTGTGTGAACA CTGTTATGGGATCTGATGCCCTCTTCTGCCATGCAGGGGCACATGGAAATTAGAGTACTCAA GTTAAAAGT CTAAAAATAAG GTAGTTCTGATGCTGTTCTGACATGACAACTGGACCTTGGTCT GTGTACAGAGATGATTGTGCGTTGTGGTTACTGGCCCTGAAA

Supplemental Table 4. Weekly and daily prednisone regimens exert opposing effects on nutrient disposal and insulin sensitivity in *mdx* mice (4-week treatment).

	vehicle	daily prednisone		weekly prednisone	
SERUM	<i>mean ± s.e.m</i>	<i>mean ± s.e.m</i>	<i>P value vs vehicle</i>	<i>mean ± s.e.m</i>	<i>P value vs vehicle</i>
corticosterone (ng/ml)	181 ± 1.01	127 ± 5.34	<0.0001	194 ± 5.05	0.118
insulin (ng/ml)	1.64 ± 0.09	3.09 ± 0.14	<0.0001	1.73 ± 0.07	0.820
BCAA (μM)	572 ± 25.3	657 ± 24.2	0.037	457 ± 14.1	0.005
free fatty acids (μM)	462 ± 11	546 ± 13.5	0.002	386 ± 17.3	0.005
TISSUE BCAA (nmol/mg)					
Quadriceps	105 ± 3.37	118 ± 2.74	0.019	89.6 ± 3.06	0.008
Diaphragm	51.6 ± 1.51	64 ± 3.09	0.002	43.8 ± 0.93	0.045
Heart	2.03 ± 0.08	2.38 ± 0.09	0.017	1.65 ± 0.07	0.012
omental fat	23.9 ± 1.32	28.2 ± 0.99	0.035	18.1 ± 0.94	0.005
TISSUE FREE FATTY ACIDS (nmol/mg)					
Quadriceps	2.26 ± 0.1	4.11 ± 0.11	<0.0001	1.25 ± 0.07	<0.0001
Diaphragm	1.78 ± 0.07	2.07 ± 0.09	0.021	1.11 ± 0.07	<0.0001
Heart	0.776 ± 0.06	0.86 ± 0.03	<0.0001	0.44 ± 0.02	<0.0001
omental fat	5.08 ± 0.1	6.01 ± 0.3	0.008	4.35 ± 0.07	0.038

Supplemental Table 5. Long-term weekly prednisone boosts disposal of BCAA and free fatty acids in circulation and peripheral tissues of *mdx* and *Dysf-null* mice.

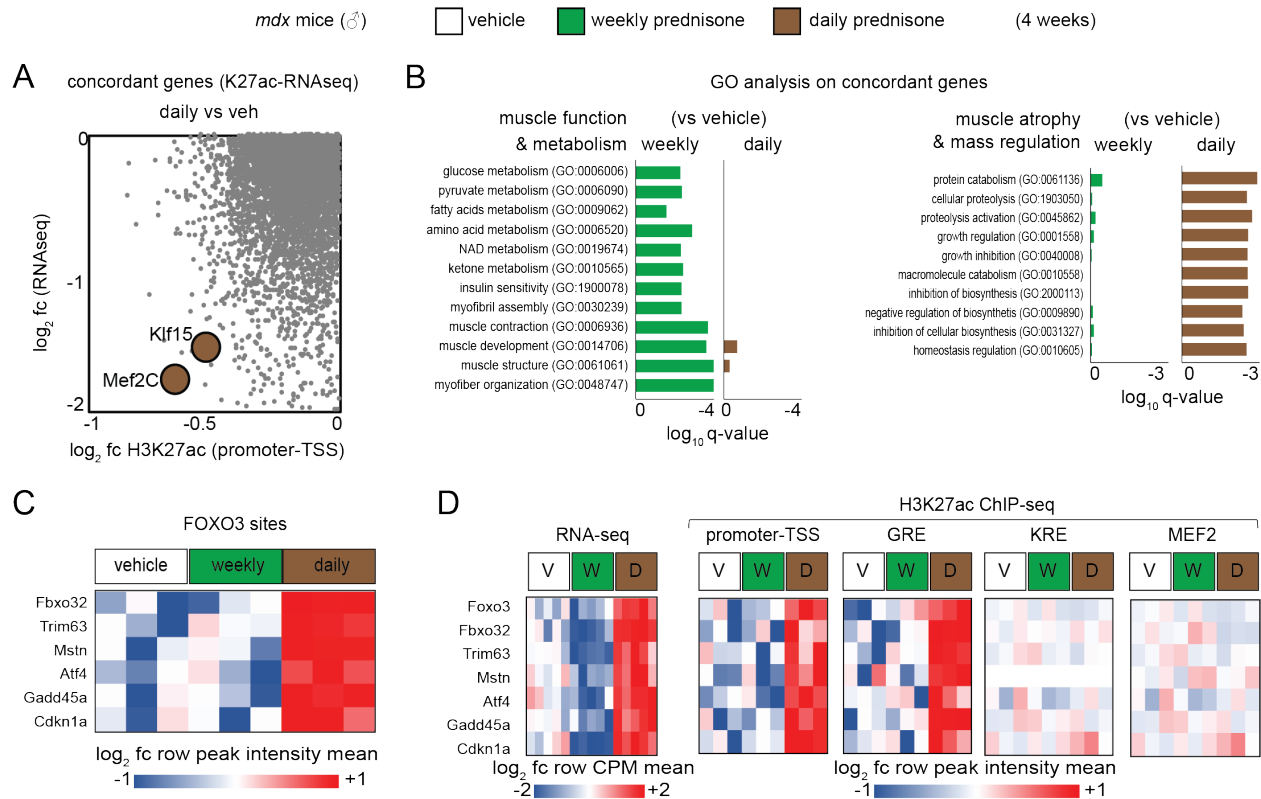
<i>mdx</i> mice (40 week-treatment)	vehicle	weekly prednisone	
BLOOD and SERUM	<i>mean ± s.e.m</i>	<i>mean ± s.e.m</i>	<i>P value</i>
creatinine kinase (U/ml)	5.42 ± 0.4	3.1 ± 0.16	0.001
insulin (ng/ml)	1.3 ± 0.1	1.51 ± 0.14	0.219
corticosterone (ng/ml)	150 ± 10.6	133 ± 8.36	0.228
BCAA (μM)	647 ± 26	462 ± 7.32	<0.0001
free fatty acids (μM)	629 ± 13.5	547 ± 10.4	0.001
TISSUE BCAA (nmol/mg)			
quadriceps	118 ± 2.3	95.3 ± 3.21	<0.0001
diaphragm	57.5 ± 2.9	49.4 ± 2.14	0.037
heart	2.46 ± 0.05	1.74 ± 0.08	<0.0001
omental fat	31.3 ± 1.46	23.5 ± 0.43	0.001
TISSUE FREE FATTY ACIDS (nmol/mg)			
quadriceps	2.05 ± 0.08	0.752 ± 0.05	<0.0001
diaphragm	2.4 ± 0.07	1.46 ± 0.05	<0.0001
heart	0.739 ± 0.03	0.211 ± 0.01	<0.0001
omental fat	4.54 ± 0.21	3.91 ± 0.12	0.019

<i>Dysf-null</i> mice (32 week-treatment)	vehicle	weekly prednisone	
BLOOD and SERUM	<i>mean ± s.e.m</i>	<i>mean ± s.e.m</i>	<i>P value</i>
creatinine kinase (U/ml)	2.42 ± 0.08	1.31 ± 0.04	<0.0001
fasting glycemia (mg/dl)	114 ± 3.51	109 ± 3.17	0.228
insulin (ng/ml)	1.26 ± 0.1	1.22 ± 0.11	0.815
corticosterone (ng/ml)	149 ± 6.08	143 ± 5.2	0.446
BCAA (μM)	519 ± 12.7	419 ± 9.95	<0.0001
free fatty acids (μM)	543 ± 11.7	475 ± 9.18	0.001
TISSUE BCAA (nmol/mg)			
quadriceps	107 ± 3.46	90.9 ± 2.58	0.002
diaphragm	51.3 ± 1.82	45.4 ± 1.06	0.014
heart	1.89 ± 0.04	0.91 ± 0.03	<0.0001
omental fat	35.2 ± 0.81	24.5 ± 0.8	<0.0001
TISSUE FREE FATTY ACIDS (nmol/mg)			
quadriceps	2.98 ± 0.24	1.05 ± 0.06	<0.0001
diaphragm	1.7 ± 0.26	0.753 ± 0.07	0.005
heart	0.69 ± 0.04	0.438 ± 0.05	0.001
omental fat	6.69 ± 0.31	3.49 ± 0.38	<0.0001

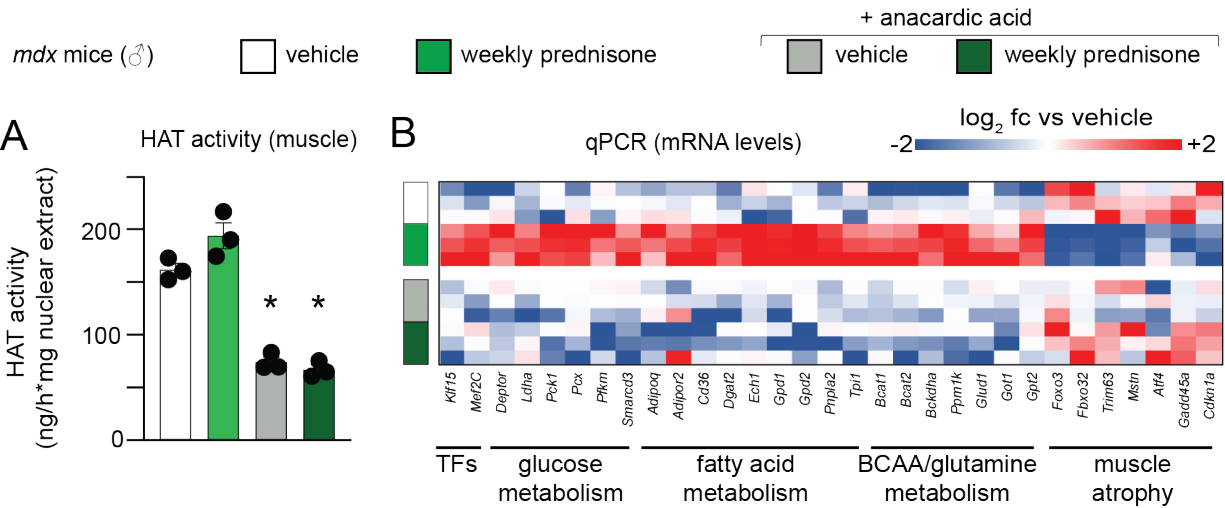
Supplemental Table 6. List of primers for ChIP-qPCR analyses.

Gene	Regulatory region	Primer F	Primer R
<i>Klf15</i>	GRE	CCTCCGTTTCTATCGGTTCA	GAACGGTCACACAAATGCAG
<i>Klf15</i>	KRE	TGTCACAGGGATGTGCCTAA	GACAAGCATCTCTGGCCTTC
<i>Klf15</i>	MEF2	ACCCTCCAGCCTATGCCTAT	GCACTCTGACTGTGCTCTGG
<i>Mef2c</i>	GRE	GATAGGGTGGAGAACGTGGA	AATCCAAACCCAGGGAAAC
<i>Mef2c</i>	KRE	AACGCAGACCTCACAGACCT	AGTGGGTGTGCTTTGGAAAC
<i>Mef2c</i>	MEF2	GTGCCATGTGCTCTGAGAAA	GCACAGCTCAGTTCCCAAAT
<i>Bcat1</i>	GRE	CAGGCCCCAGCTATTACTGA	TCTCAGCTTTAGGGGTGGAG
<i>Bcat1</i>	KRE	ATTGCCATGATTCAACACGA	GCGGGAATGCCATAGTTTAT
<i>Bcat1</i>	MEF2	ACCCAGCTGCTCAGTCAAAT	TTTCACATGAAAGCCACAGC
<i>Bckdha</i>	GRE	AACTGAACCTGGGACCTTCA	GAACATGCGTGCTTGAAGA
<i>Bckdha</i>	KRE	GGAAATTGGCAGCAGAGGTA	ATCCATGTCCCTGCACATCT
<i>Bckdha</i>	MEF2	TCGGTGACAATGAGCAGAAG	ATGCATGCAGACAGAACACC
<i>Glud1</i>	GRE	GTGCCAGCCTGGACTACATA	CACCCACCACAACACAGAT
<i>Glud1</i>	KRE	AGGGGCCTGGTGACTCAT	CTTTGCAGATGGGCTTGGT
<i>Glud1</i>	MEF2	ATCGGCTCTCCAGTGTTTA	GATTGCAGCAAGTCACCAGA
<i>Got1</i>	GRE	GTGGGGAAGCAGAGAACAG	CTTTCTGGGGAAGCACTGAG
<i>Got1</i>	KRE	GTGATGTGGGCATGGATGTA	CATGTGCTTCTGGAACAGGA
<i>Got1</i>	MEF2	GACTGGAGGTTTTCTGTGC	GGCCTTTGTGGTGACTTGAT
<i>Gpt2</i>	GRE	CCTTCGACGGTTCACTTGT	CCCCTTCGTCTCACTTCAAA
<i>Gpt2</i>	KRE	GGGGCACCTAATGTCTCTT	TGCAAAACCTGTGTCAAAA
<i>Gpt2</i>	MEF2	GTGGGTCTCAACCTCTTGG	GGAGCTTCAGGATTGTCTGC
<i>Deptor</i>	GRE	CAGTGGTGCAAAGTGAATGG	TGGGTCTTCACACCACTGAA
<i>Deptor</i>	KRE	GGTCTGTGGAAGAAGCCAAG	AACGAAATTGGTCAGGTTGG
<i>Deptor</i>	MEF2	CCCTTAACCAAAAGCAACCA	GGGAAGCTTGGGCTAATAGG
<i>Ldha</i>	GRE	TATGTGACCATGCCTTGGA	TGAGCTGACAGACAGGTGCT
<i>Ldha</i>	KRE	ATCTCCAGAGCAAAGGACGA	CCCCAGTTCAGAAACCAGAA
<i>Ldha</i>	MEF2	CAGACTTGAGGTTTGCGTGA	GACAAGATCTCTGGGCAAGC
<i>Pck1</i>	GRE	CCTGGAAGAACAGGAGTGG	CTACGGCCACCAAGATGAT
<i>Pck1</i>	KRE	ATCATCTTTGGTGGCCGTAG	CCAGAGAAGCCATTGGTGAT
<i>Pcx</i>	KRE	AGCCAATCAGGATGAGCTTC	ACCTACCCCTCGCGTTTAAAG
<i>Pcx</i>	MEF2	CGTGCCTAAGTACCCCTTT	CAGGGAGATCTTGCCATTGT
<i>Pfkm</i>	GRE	ATTAGCAACCATGGCCACTC	CACTGAGGAAGGCTGTGTGA
<i>Pfkm</i>	KRE	GCCATCCAGACTGATTCCAT	GTGTGAAGAGCAGGCTTGG
<i>Pfkm</i>	MEF2	TGCACCTATGATGCTTCCAG	CAAGAGGCACAGGACACAAA
<i>Smarcd3</i>	GRE	CCCTCGCCACAAATAGTTTC	CCAGATTCTTCCAGCAAAT
<i>Smarcd3</i>	KRE	AGAATGACTTGGTCGCTGCT	GCCTGTTTCTGCTTCACCTC
<i>Smarcd3</i>	MEF2	CTGTGTGCTTCCCTTCACAA	ATTTCCTTATTGCCCTCAC
<i>Adipoq</i>	GRE	CCTGCTGGCTCTGAGACATT	CTGCAAGACACTCCCTGGAT
<i>Adipoq</i>	KRE	CAGGAGGACTGCAGACAAGA	CTTTGGTACCATCGCAACCT
<i>Adipoq</i>	MEF2	CTGCATTCCCCAAATTAAT	GGCACATTGGTCTTGATTTC
<i>Adipor2</i>	GRE	TTTTCTTCTCCCTCTGGAA	ACCAAAACCAACAACCAAA
<i>Adipor2</i>	KRE	CGGATTCTGTGTTGTGTGG	ACACTTGAGAGGCAGGTGCT
<i>Adipor2</i>	MEF2	TTGGTTTCTCTGCCCTTTTG	GACACAGCGAATTGCTCTCA
<i>Cd36</i>	GRE	TGACATTGCTGGGAATTGAA	TGGGATTGTAGACCAGTTTGC
<i>Cd36</i>	KRE	CTACCGGGCGTTGTTCTAAA	ACCGTTCCCATAGACACTGG
<i>Cd36</i>	MEF2	TCAACCATGTGCTGATATTGAC	CCCTCCTTCTCGAAATGTT
<i>Dgat2</i>	GRE	GGGTCTCTTAGGACCACCAA	ACTGCAAGCAGACACACGAG
<i>Dgat2</i>	KRE	GCCACCTAGATGAGCAGAA	CACCCCTACAAGAACATGG
<i>Dgat2</i>	MEF2	TGAAAAAGTGGGCTGGAGAG	CCCTCATCCCAACTGTCT
<i>Ech1</i>	GRE	GCTTGAGTGACAGTGTGT	CCTGCTCTGGAGTGGAGAAC
<i>Ech1</i>	KRE	AGGGTGTCTTTCTGCTCAC	CAGTGGGACAGTAGGGGATG
<i>Ech1</i>	MEF2	TGCAAGCCTTCAAACCTCT	GACCTTTGGAAGAGCAGTCG
<i>Gpd1</i>	GRE	AGGGTAGGAAATGCCCTCAG	AAGGCAACAGCACTCTGCTC
<i>Gpd1</i>	KRE	CCTGTTCACACAGGAAGGT	GGGGGAGGAACATCAAAAGC
<i>Gpd2</i>	GRE	GGTGCTCATGGGTTTCTGAT	GTCCATGCTGACTTCCCACT
<i>Gpd2</i>	KRE	GGTGCTCATGGGTTTCTGAT	GTCCATGCTGACTTCCCACT
<i>Gpd2</i>	MEF2	TTCTCCCTCCAAAATGTCTCA	CCCCAAGGAAAAGAACAACA
<i>Pnpla2</i>	GRE	GCCACACTTCTGTGCTTTGA	CCGCAGAAAACCTAGACAA
<i>Pnpla2</i>	KRE	GGTCTCTCAGATGGCTTTGC	AGGCAGAGGAGGAGGTGTTT
<i>Pnpla2</i>	MEF2	GTTCTTGGCACCAGCATCTC	CCAGGGCTTATCTGGTACA
<i>Tpi1</i>	KRE	GTTTGCTCGAACACGACCTT	CTGGGGCACTCAGAAAAGAG
<i>Tpi1</i>	MEF2	CCTTCCAATGCCTCTGATA	GATCATCCATTCCCAAGA

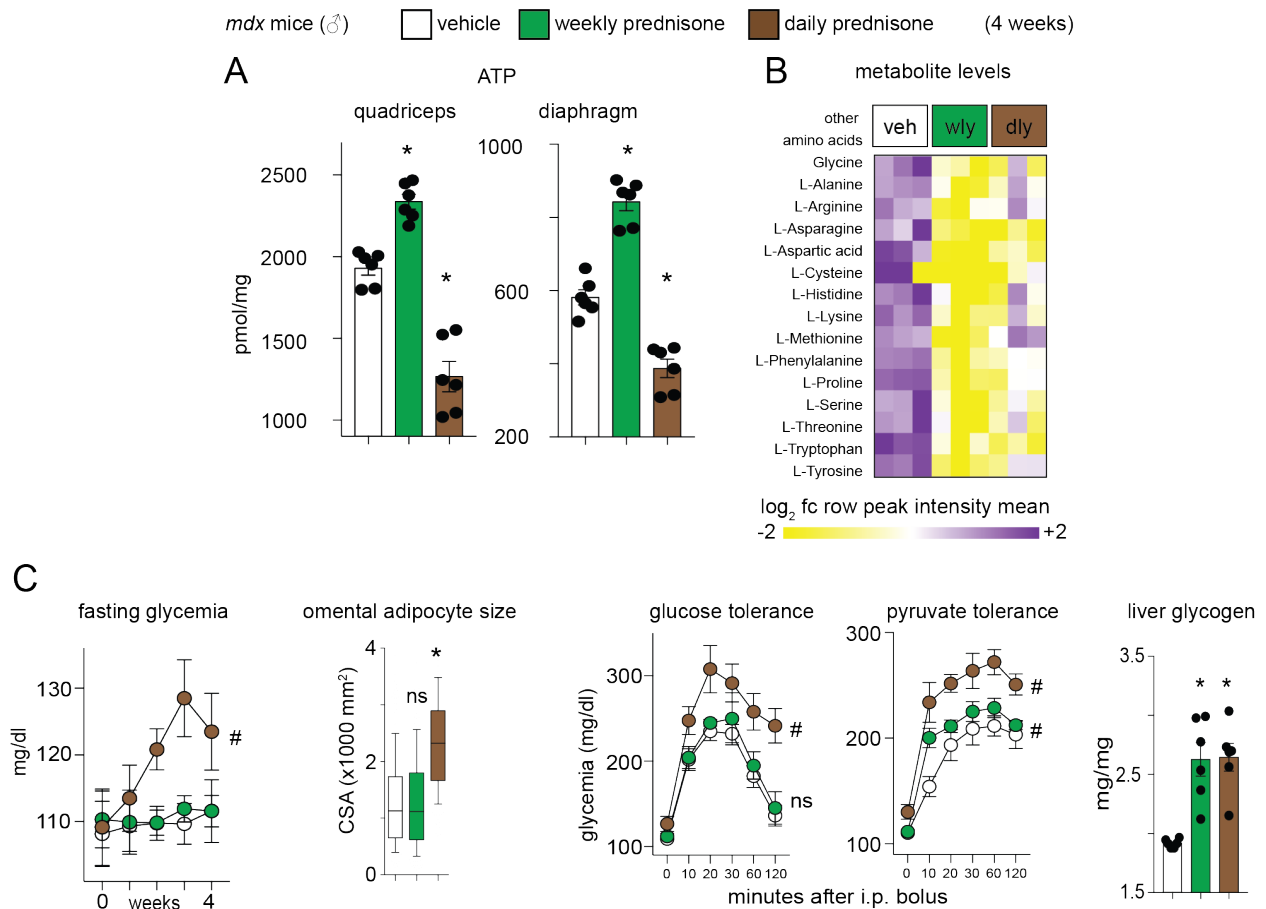
SUPPLEMENTAL FIGURES



Supplemental Figure 1. Divergent epigenomic and transcriptomic programs elicited by glucocorticoid regimens in dystrophic muscle. (A) After daily prednisone, *Klf15* and *Mef2C* showed reduced expression and H3K27 acetylation in treated *mdx* myofibers. (B) Genes with both increased expression and H3K27Ac marks were identified. Gene ontology (GO) analysis of these concordant genes showed that weekly prednisone enriched for nutrient metabolism and muscle function pathways, while daily prednisone exposure enriched for atrophy-related terms. (C) Daily prednisone drives atrophy pathways seen as enrichment for FOXO3 sites marked with increased H3K27ac marks. (D) Pathway-centered analysis showed that GRE but not KRE or MEF2 sites on atrophy genes were activated after daily prednisone. N=3 mice/group for K27ac ChIP-seq, n=5 mice/group for RNAseq.



Supplemental Figure 2. Anacardic acid administration reduced histone acetyl-transferase (HAT) activity in muscle and blunted transcriptional gains in nutrient metabolism pathways induced by weekly prednisone. (A) Muscle HAT activity was significantly reduced at endpoint of i.p. anacardic acid administration. **(B)** qPCR analyses showed loss of gene upregulation in muscles co-treated with weekly prednisone and anacardic acid. Histograms depict single values and mean \pm s.e.m.; n=3 mice/group *, P<0.05 vs vehicle, 1-way ANOVA test with Tukey's multiple comparison.



Supplemental Figure 3. Divergent metabolic programs elicited by pulsatile weekly versus daily prednisone in *mdx* mice. (A) ATP levels were increased in both locomotory (quadriceps) and respiratory (diaphragm) muscles compared to vehicle treated, while daily prednisone reduced ATP content in both muscles. (B) Weekly prednisone treatment induced a general trend in lower levels of free amino acids in muscle, as quantitated through metabolomic analysis. (C) Daily, but not weekly, prednisone induced hyperglycemia, adipocyte hypertrophy, and glucose intolerance. However, both regimens seemingly upregulated liver gluconeogenesis, as observed through pyruvate tolerance tests and liver glycogen levels. Curves depict mean \pm s.e.m.; histograms depict single values and mean \pm s.e.m.; box plots, Tukey distribution; n=6 mice/group (A, C), n=3 mice/group (B). *, P<0.05 vs vehicle, 1-way ANOVA test with Tukey's multiple comparison; #, P<0.05 vs vehicle, 2-way ANOVA test.

SUPPLEMENTAL METHODS

RNA-seq. RNA-seq datasets used for analyses in this work can be accessed on the NCBI GEO database (GSE95682). Total RNA was purified from ~30mg quadriceps muscle tissue of treated and control DBA/2J-*mdx* male 6 month-old mice with the RNeasy Protect Mini Kit (Cat #74124; Qiagen, Hilden, Germany) as per manufacturer's instructions. RNA quantity and quality were respectively analyzed with Qubit fluorometer (Cat #Q33216; Thermo Fisher Scientific, Waltham, MA) and 2100 Bioanalyzer (Cat #G2943; Agilent Technologies, Santa Clara, CA). Libraries were prepared from approximately 1mg RNA/sample with TruSeq Stranded Total RNA Library Prep Kit (Cat #RS-122-2203; Illumina, San Diego, CA). Libraries were sequenced through the NextSeq 500 System (high-throughput, paired-end 150bp fragment sequencing; #SY-415-1001; Illumina, San Diego, CA). Raw reads were aligned with TopHat v2.1.0 to the mm10 genome assembly (gcm38, version 78) (60). Transcripts were assessed and raw read counts per gene were quantified with HTseq (61). Reads Per Kilobase of transcript per Million mapped reads (RPKM) and fold-changes between groups were calculated using EdgeR from the Bioconductor package (62). Differentially expressed genes were identified by adjusted P-value <0.05. Heatmaps were visualized with GiTools (63).

ChIP-qPCR and RT-qPCR. For ChIP-qPCR assays, chromatin was immunoprecipitated following the procedures detailed for ChIP-seq, and then assayed in three replicates using 1X Sybr Green iTaq mix (Cat #1725125; Bio-Rad, Hercules, CA) and 100nM primer mix (**Supp Table 6**) at a CFX96 qPCR machine (Bio-Rad, Hercules, CA; thermal profile: 95C, 10sec; 60C, 20sec; 72C, 30sec; 60X; melting curve). Quantitation was performed as % of input, and IgG-immunoprecipitated chromatin was assayed as negative control. Primary antibodies: rabbit anti-H3K27ac (Cat #39133, Active Motif, Carlsbad, CA), rabbit anti-GR, -KLF15, -MEF2C (Cat #2164; #7194; #2585; ABclonal, Woburn, MA), rabbit IgG (Cat #ab27472, Abcam, Cambridge, MA). For qPCR assays, total mRNA was extracted using Trizol (Cat #15596026; Thermo Fisher Scientific, Waltham, MA) from cryo-pulverized quadriceps muscles, and 1µg RNA was reverse-transcribed using 1X qScript Supermix (Cat #95048; QuantaBio, Beverly, MA). 1:10-diluted cDNA was assayed with Sybr Green iTaq mix as detailed above (thermal profile: 95C, 10sec; 60C, 20sec, 72C, 30sec; 40X; melting curve). Primers were selected among validated primer sets from the MGH PrimerBank; IDs: 12963561a1, 20070856a1, 26331298a1, 33859514a1, 31982494a1, 30425290a1, 6680027a1, 6754034a1, 27805389a1, 21703930a1, 6754524a1, 7110683a1, 6679237a1, 31981185a1, 31981140a1, 31982423a1, 23271651a1, 31982474a1, 16975490a1, 7949037a1, 6753966a1, 31981769a1, 6678678a1, 26327465a1, 6678413a1, 10946948a1, 10442021a1, 21362329a1, 9789951a1, 13385848a1, 21523717a1, 6754752a1, 6753128a1, 6681149a1, 6671726a1.

Metabolic cages. VO₂ (ml/h/kg) and energy expenditure to body weight (kcal/h/kg) were assessed via indirect calorimetry using the TSE Automated Phenotyping System PhenoMaster (TSE system, Chesterfield, MO). Mice were singly housed in their home cages in an enclosed environmental chamber (part of the TSE system) with controlled temperature and light/dark cycles (12 hours each; 6AM-6PM). After a three-day period of acclimation to the metabolic chamber, data collection started at 48 hours after prednisone or vehicle injection and lasted for 5 days. Measurements of CO₂ production and O₂ consumption occurred using the attached gas analyzer to assess energy expenditure. In addition, physical activity in three dimensions was monitored via infrared beam breaks through frames mounted on the perimeter of the metabolic cages. Enrichment items were omitted to avoid insulation from sensors and infrared light beam path obstruction. Results are expressed as 12 hour-period values (light/dark; 10 values per mouse). Metabolic cage assays were conducted blinded to treatment groups.

Muscle function, whole-body plethysmography, echocardiography. Forelimb grip strength was monitored using a meter (Cat #1027SM; Columbus Instruments, Columbus, OH) blinded to treatment groups. Animals performed ten pulls with 5 seconds rest on a flat surface between pulls. Immediately before sacrifice, *in situ* tetanic force from *tibialis anterior* muscle was measured using a Whole Mouse Test System (Cat #1300A; Aurora Scientific, Aurora, ON, Canada) with a 1N dual-action lever arm force transducer (300C-LR, Aurora Scientific, Aurora, ON, Canada) in anesthetized animals (0.8 l/min of 1.5% isoflurane in 100% O₂). Tetanic isometric contraction was induced with following specifications: initial delay, 0.1 sec; frequency, 200Hz; pulse width, 0.5 msec; duration, 0.5 sec; using 100mA stimulation (64). Length was adjusted to a fixed baseline of 50mN resting tension for all muscles/conditions. Fatigue analysis was conducted by repeating tetanic contractions every 10 seconds until complete exhaustion of the muscle (50 cycles). Time of contraction was assessed as time to max tetanic value within the 0.0-0.5 sec range of each tetanic contraction, while time of relaxation was assessed as time to 90% min tetanic value within the 0.5-0.8 sec range of every tetanus. Unanesthetized whole-body plethysmography (WBP) was used to measure respiratory function using a Buxco Finepointe 4-site apparatus (Data Sciences International, New Brighton, MN). Individual mice were placed in a calibrated cylindrical chamber at room temperature. Each mouse was allowed to acclimate to the plethysmography chamber for 120 minutes before recording was initiated. Data was recorded for a total of 15 minutes broken into 3 consecutive 5-minute periods. All physiological studies were conducted blinded to treatment groups. Cardiac function was assessed by echocardiography, which was conducted under anesthesia (0.8L/min of 1.5% vaporized isoflurane in 100% O₂) on mice between 2 and 5 days before sacrifice. Echocardiography was performed using a Visual Sonics Vevo 2100 imaging system with an MS550D 22-55 MHz solid-state transducer (FujiFilm, Toronto, ON, Canada). Longitudinal and circumferential strain measurements were calculated using parasternal long-axis and short-axis B-mode recordings of three consecutive cardiac cycles, analyzed by the Vevo Strain software (FujiFilm, Toronto, ON, Canada). Recording and analysis were conducted blinded to treatment group.

Multi-modal imaging (FDG-PET, microCT, MRI). Mice were anesthetized in an induction chamber with 3% isoflurane in oxygen, weighed, and then transferred to a dedicated imaging bed with isoflurane delivered via nosecone at 1-2%. Mice were placed in the prone position on a plastic bed and immobilized to minimize changes in position between scans. Respiratory signals were monitored using a digital monitoring system developed by Mediso (Mediso-USA, Boston, MA). Mice were imaged with a preclinical microPET/CT imaging system (nanoScan PET/CT, Mediso-USA, Boston, MA). CT data was acquired with a 2.2x magnification, <60 μ m focal spot, 2 \times 2 binning, with 480 projection views over a full circle, using 50 kVp/520 μ A, with a 300 ms exposure time. The projection data was reconstructed with a voxel size of 250 μ m and using filtered (Butterworth filter) backprojection software from Mediso. A bone mineral density standard (GRM GmbH, Moehrendorf, Germany) with hydroxyapatite (HA) from 0 to 1200 mg HA/cm³ was used to convert the CT images from Hounsfield units to bone mineral density. The HA standard was imaged with the same parameters. For PET imaging, a target of 10 MBq of ¹⁸F-fluorodeoxyglucose (FDG) was injected intravenously after mice had been fasted for four hours. PET acquisition parameters were as follows: 1:1 coincidence detection and 30-minute acquisition time. MLEM reconstruction was used with CT for attenuation correction and scattering. Pixel size was set to 0.3 \times 0.3 mm. Mice were fasted overnight prior to imaging in the early morning (~8AM). After completion of PET/CT, each mouse was transferred to the MRI scanner and a reference standard consisting of one tube of canola oil and one tube of water was positioned above its back. MRI was performed on a 9.4T Bruker Biospec MRI system with a 30 cm bore, a 12 cm gradient insert, and an AutoPac laser positioned motorized bed (Bruker Biospin Inc, Billerica, MA). Respiratory signals and temperature were monitored using an MR-

compatible physiologic monitoring system (SA Instruments, Stonybrook, NY); a warm water circulating system was used to maintain body temperature. A 72mm quadrature volume coil (Bruker Biospin, Inc, Billerica, MA) was used to image each mouse's whole body in two overlapping fields of view. First, the mouse was positioned with the thorax at the magnet's isocenter and imaged using a T₁-weighted accelerated spin echo sequence (Rapid Acquisition with Relaxation Enhancement, RARE) with five pairs of interleaved axial slice stacks covering brain to mid-abdomen. TR was nominally set at 1000 ms; with respiratory gating the functional TR was approximately 1500 ms (range 1300-2000 ms). The following additional parameters were used: TE = 6.25 ms, RARE factor 4, MTX = 256 x 256, FOV 45 x 45 mm, 15 slices of 1 mm thick, 4 mm gap between slices, and 2 signal averages. Each image stack was acquired with and without fat saturation. Acquisition time was approximately 3 minutes per scan. After imaging the upper portion of the mouse, the imaging bed was moved deeper into the magnet and two more pairs of interleaved image stacks were acquired to cover the lower abdomen and legs. Parameters were the same as above, except for a 1 mm gap between slices and 3 signal averages. The reconstructed data was visualized in Amira 6.5 (FEI, Houston, TX). The interleaved MRI stacks for upper body and lower body were individually merged, then normalized to the water signal from the reference standard. Then the upper and lower body stacks were registered to each other using a combination of normalized mutual information and manual registration, and merged to create whole body fat-suppressed and non-fat-suppressed MR images. A difference (fat only) image was created by subtracting the normalized fat-suppressed image from the normalized non-fat-suppressed image and segmented by thresholding (using the water and canola oil references as a guide). A small amount of manual segmentation was necessary in regions near the testes where fat suppression pulses were less effective. CT images were registered to the MRI data using normalized mutual information. The fat region of interest (ROI) was used in both the MRI data and FDG-PET data for quantitative analysis. Additionally, each leg was segmented into its own ROI for FDG-PET analysis using the MRI images without fat saturation. A skeleton ROI was generated for each mouse by using a 750 HU threshold in the CT image. The % injected dose (%ID) of FDG in fat and muscle tissue was calculated by dividing the total PET signal found in the ROI with the total PET signal in a mouse whole-body ROI. Mass of body fat was determined by multiplying the volume of fat ROIs with the average density of adipose tissue (0.92 g/cm³) (65). The HA standard was segmented with ROIs of 0, 50, 200, 800, and 1200 mg/cm³ and used to create a linear correlation between HU and bone density with a r² of 0.99.

CK dosing. Serum creatine kinase (CK) was analyzed in triplicate for each mouse using the EnzyChrom Creatine Kinase Assay (Cat # ECPK-100; BioAssay Systems, Hayward, CA) following manufacturer's instructions. Results were acquired with the Synergy HTX multi-mode plate reader (BioTek®, Winooski, VT) and expressed as U/ml for murine and U/l for human samples. Both HOP and CK dosing assays were conducted blinded to treatment groups.

Histology. Excised tissues (muscles, omental fat, heart) were placed in 10% formaldehyde (Cat #245-684; Fisher Scientific, Waltham, MA) for histologic processing. Seven µm sections from the center of paraffin-embedded muscles were stained with hematoxylin and eosin (H&E; cat #12013B, 1070C; Newcomer Supply, Middleton, WI) and Masson's trichrome (Cat #HT-15; Sigma-Aldrich; St. Louis, MO). Myofiber/adipocyte CSA quantitation was conducted on 400 myofibers/adipocytes per tissue per mouse. Imaging was performed using a Zeiss Axio Observer A1 microscope, using 10X and 20X (short-range) objectives. Brightfield pictures were acquired via Gryphax software (version 1.0.6.598; Jenoptik, Jena, Germany). Area quantitation was performed by means of ImageJ (59). Sample processing, imaging and CSA quantitation were conducted blinded to treatment groups.

Protein analysis. Protein lysates from ~50mg muscle tissue were obtained with homogenization at the TissueLyser II (cat #85300; Qiagen, Hilden, Germany) for two rounds of 2 minutes each with 2 minutes pause in between, using sample plates chilled at -20°C o/n and one stainless 5mm bead per sample (cat#69989; Qiagen, Hilden, Germany). Each tissue was homogenized in 250µl RIPA buffer (cat #89900, Thermo Scientific, Waltham, MA) supplemented with protease and phosphatase inhibitors (cat #04693232001 and #04906837001, Roche, Basel, Switzerland). Homogenized samples were then sonicated for 15 cycles (30 sec, high power; 30 sec pause; 200µl volume) in a water bath sonicator set at 4°C (Bioruptor 300; Diagenode, Denville, NJ) and ~10µg protein lysate was mixed with 1:1 volume of 2x Laemmli buffer (cat#161-0737; Bio-Rad, Hercules, CA) and incubated at 95°C for 15 minutes. Protein electrophoresis was performed in 4-15% gradient gels (cat#456-1086; Bio-Rad, Hercules, CA) in running buffer containing 25mM TRIS, 192mM glycine, 0.1% SDS, pH 8.3. Proteins were then blotted on 0.2µm PVDF membranes (cat#16220177; Bio-Rad, Hercules, CA), previously activated for 3 minutes in 100% methanol, in transfer buffer containing 25mM TRIS, 192mM glycine, 20% methanol at 300mA for ~3.5 hours at 4°C. Membranes were washed with TBS-T buffer containing 20mM TRIS, 150mM NaCl, 0.1% Tween-20, pH 7.6, and then blocked with StartingBlock (cat#37543, Thermo Scientific, Waltham, MA). Primary antibody incubation was performed o/n at 4°C with the following antibodies: rabbit anti-phospho BCKDHA (ser293; cat#A304-672A-T), anti-total BCKDHA (cat#A303-790A-T), rabbit anti-mTOR (cat#A301-143A-T), rabbit anti-RagC (cat# A304-299A-T), rabbit anti-S6K (cat# A300-510A-T), rabbit anti-4EBP1 (cat# A300-501A-T; Bethyl Laboratories, Montgomery, TX); rabbit anti-phospho-S6K (Thr389; cat# AP0564), rabbit anti-phospho-4EBP1 (Ser65; cat# AP0032; ABclonal, Woburn, MA); mouse anti-myosin heavy chain (cat# MF20), mouse anti-puromycin (cat#PMY-2A4; DSHB, Iowa City, IA). Secondary antibody incubation was performed at room temperature for 1 hour with the following antibodies: donkey anti-rabbit and anti-mouse (cat#sc-2313 and #2314; Santa-Cruz Biotechnology; Dallas, TX). Blots were developed with SuperSignal Femto (cat#34096; Thermo Scientific, Waltham, MA) using the iBrightCL1000 developer system (cat #A32749; Thermo Scientific, Waltham, MA) with automatic exposure settings. Protein density was analyzed using the Gel Analysis tool in ImageJ software (59). Only bands from samples run and blotted in parallel on the same gels/membranes were analyzed for ratios. Phosphorylation levels were quantitated as ratio versus total protein; co-IP levels were quantitated as ratio versus bait protein; total protein levels were quantitated as ratio to housekeeping/structural protein control. Image acquisition and densitometric analysis were conducted blinded to treatment group.

Supplemental References

60. Trapnell C, Pachter L, Salzberg SL. TopHat: discovering splice junctions with RNA-Seq. *Bioinformatics*. 2009;25(9):1105–1111.
61. Anders S, Pyl PT, Huber W. HTSeq--a Python framework to work with high-throughput sequencing data. *Bioinformatics*. 2015;31(2):166–169.
62. Robinson MD, McCarthy DJ, Smyth GK. edgeR: a Bioconductor package for differential expression analysis of digital gene expression data. *Bioinformatics*. 2010;26(1):139–140.
63. Perez-Llamas C, Lopez-Bigas N. Gitools: analysis and visualisation of genomic data using interactive heat-maps. *PLoS ONE*. 2011;6(5):e19541.
64. Quattrocchi M, et al. Mesodermal iPSC-derived progenitor cells functionally regenerate cardiac and skeletal muscle. *J Clin Invest*. 2015;125(12):4463–4482.
65. Hill AM, LaForgia J, Coates AM, Buckley JD, Howe PR. Estimating abdominal adipose tissue with DXA and anthropometry. *Obesity (Silver Spring)*. 2007;15(2):504–510.